Structures, Energetics, and Chemical Reactions of Anions Derived from Cyclooctatetraene

Shuji Kato, Roustam Gareyev, Charles H. DePuy, and Veronica M. Bierbaum*

Contribution from the Department of Chemistry and Biochemistry, University of Colorado, Boulder, Colorado 80309-0215

Received July 31, 1997

Abstract: Structures, energetics, and reactions of anions derived from cyclooctatetraene [$C_8H_8^-$ (**1**), $C_8H_7^-$ (**2**α), and $C_8H_6^-$ (**3**)] have been studied using the selected ion flow tube (SIFT) technique and molecular orbital (MO) calculations. Radical anions **1** and **3** undergo electron detachment upon collisional excitation with helium whereas anion **2**α undergoes a remarkable rearrangement to an isomeric species, $C_8H_7^-$ (**2***β*). The anion **2**α is not a vinylic species but rather a novel structure incorporating a *π*-electronic system and an allenic moiety within the eight-membered ring. The anion **2***β* is a relatively stable [3.3.0] bicyclic species with a proton affinity and electron binding energy very similar to those for cyclopentadienide ion. The molecular structures are predicted and the mechanisms of isomerization are elucidated using MO calculations. Bimolecular reactions of these anions are thoroughly examined with NO, NO_2, SO_2, COS, CS_2, and O_2. The reactivity of **2**α is interpreted in terms of the high proton affinity and the strain of the allenic bond. Anion **3** exhibits a remarkable reaction with NO to yield CN^-. The adiabatic electron affinity of cyclooctatetraene has been unambiguously determined as 0.55 ± 0.02 eV from equilibrium measurements with the SIFT technique. Heats of formation for the anions and their corresponding neutrals, along with the homolytic C−H bond dissociation energies for the conjugate acids, have also been determined.

Introduction

Conformational changes in 1,3,5,7-cyclooctatetraene (COT) and its substituted derivatives have been the subject of considerable interest for several decades. The COT molecule is a tublike, eight-membered ring with alternating double bonds, and its structural flexibility affords a variety of dynamic processes: ring inversion, bond shifting, and valence isomerization.[1,2] Many kinetic and thermodynamic parameters have been studied for COT and substituted COTs with the goal of addressing some of the central questions in physical organic chemistry, such as the resonance energy for a Hückel antiaromatic 4*n* system.[1,2]

Relatively little is known, however, about the structures and energetics of anionic species derived from COT. This category includes a radical anion of COT [COT^- (**1**)], which is one of the first open-shell annulenes observed experimentally, and its deprotonated and dehydrogenated anions [$C_8H_7^-$ (**2**α) and $C_8H_6^-$ (**3**)]. For the radical anion **1**, the value of the electron

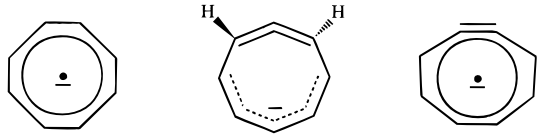

1 **2**α **3**

binding energy (EBE) has been controversial for many years.[3−5] A molecular orbital (MO) study confirmed the structure of COT^- to be planar,[6] far different from that of neutral COT. The very large conformational change between COT and COT^- has made the EBE difficult to determine. On the other hand, this conformational change provides an opportunity for accessing the transition state of COT ring inversion by electron detachment of COT^-.[5] In relation to **1** and COT, structures of **2**α (ref 7), **3** (ref 8), and their detached neutral species have been studied using photoelectron spectroscopy (PES) and MO calculations. In a recent communication, we have shown that these species have intriguing structures; anion **2**α and its detached neutral have strained allenic moieties[7] whereas radical anion **3** and its detached neutral have strained triple bonds,[8] embedded in the ring environments. In addition, anion **2**α has a novel *π*-electron configuration.[7] We have combined the selected ion flow tube (SIFT) technique, which provides access to adiabatic processes of these anions at thermal energy, with PES and MO calculations to determine a complete set of thermochemical parameters, i.e., electron affinities (EA), acidities (ΔH_{acid}), and C−H bond dissociation energies (BDE), for COT and the series of neutrals derived from COT.[7]

Anionic chemistry of large ring systems has not been extensively studied in the gas phase. The structures of these anions stimulate an interest in their chemical reactions. Novel unimolecular and bimolecular processes may be anticipated from the greater number of degrees of freedom of motion and the strained multiple bonds embedded in the ring structures. The

(1) Fray, G. I.; Saxton, R. G. *The Chemistry of Cyclooctatetraene and Its Derivatives*; Cambridge University Press: New York, 1978.
(2) (a) Paquette, L. A. *Tetrahedron* **1975**, *31*, 2855−2883. (b) Paquette, L. A. *Pure Appl. Chem.* **1982**, *54*, 987−1004. (c) Paquette, L. A. *Acc. Chem. Res.* **1993**, *26*, 57−62.
(3) Wentworth, W. E.; Ristau, W. *J. Phys. Chem.* **1969**, *73*, 2126−2133.
(4) Gygax, R.; McPeters, H. L.; Brauman, J. I. *J. Am. Chem. Soc.* **1979**, *101*, 2567−2570.
(5) Wenthold, P. G.; Hrovat, D. A.; Borden, W. T.; Lineberger, W. C. *Science* **1996**, *272*, 1456−1459.
(6) Hammons, J. H.; Hrovat, D. A.; Borden, W. T. *J. Am. Chem. Soc.* **1991**, *113*, 4500- 4505.
(7) Kato, S.; Lee, H. S.; Gareyev, R.; Wenthold, P. G.; Lineberger, W. C.; DePuy, C. H.; Bierbaum, V. M. *J. Am. Chem. Soc.* **1997**, *119*, 7863−7864.
(8) Wenthold, P. G.; Lineberger, W. C. *J. Am. Chem. Soc.* **1997**, *119*, 7772−7777.

S0002-7863(97)02628-0 CCC: $15.00
Published on Web 05/06/1998

SIFT instrument not only allows studies on bimolecular thermal energy chemistry of **1**, **2**α, and **3** but can also be used for exploring unimolecular processes [collision-induced dissociation (CID) and isomerization] by utilizing its capability of characterizing the chemical reactivities of daughter species in the reaction flow tube.

This paper is a continuation of our previous work[7] on the structures and energetics of eight-membered ring species, C_8H_n and $C_8H_n^-$ (n = 6, 7, 8). Along with the thermochemical properties, we focus on the reactivities of these anions. We demonstrate a novel, collision-induced isomerization of $C_8H_7^-$ (**2**α) to $C_8H_7^-$ (**2**β) upon SIFT injection of **2**α at elevated kinetic energies (KE) and collision with helium.

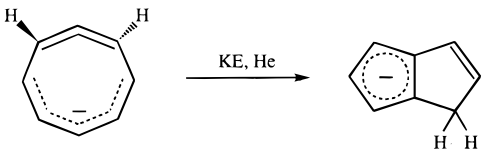

(1)

2α **2**β

The isomerization mechanism is elucidated using MO calculations. Chemical reactions of **1**, **2**α, **2**β, and **3** with NO, NO_2, SO_2, COS, CS_2, and O_2 are studied, and several novel reactions are reported.

Experimental Section

This section presents an overview of the experimental approach. Some of the details that are specific to each measurement will be described later with the results.

Reactions were studied at room temperature with the tandem flowing afterglow-selected ion flow tube (FA-SIFT) instrument, which has been described in detail elsewhere.[9] Anions were produced in the source flow tube at a helium pressure of 0.25 Torr. The $C_8H_8^-$ (**1**) ions were generated by electron attachment to COT while $C_8H_7^-$ (**2**α) and $C_8H_6^-$ (**3**) ions were formed by reactions of COT with HO^- and O^-, respectively. COT (Aldrich, 98%) was purified by distillation before use. Ions were selected by a quadrupole mass filter and injected through an orifice into the reaction flow tube maintained at 0.48 Torr of helium pressure. The SIFT injection energy, which is defined as the potential difference between the source flow tube and the injection orifice, was typically 20 eV for experiments with **1**, **2**α, and **3**. In collision-induced excitation experiments, the SIFT injection energy was varied by changing the potential on the injection orifice. The ion **2**β was produced by injecting **2**α at higher injection energies, typically at ~40 eV [at these higher energies we also observed CID of **2**α to form $C_8H_6^-$ (γ), which has a different reactivity than $C_8H_6^-$ (**3**)]. Injected ions were reacted with neutral gases added through multiple reactant inlets located along the reaction flow tube. An extra neutral inlet is attached immediately after the SIFT injection orifice and before the downstream reactant inlets. This inlet was used in experiments in which injected ions were pretreated with different gases before being subjected to reactions of interest in the flow tube. Parent and product ions were analyzed with a detection quadrupole mass filter at the end of the flow tube.

In reaction rate measurements, the multiple reactant inlets were used to vary the reaction distance in the flow tube. Absolute reaction rate constants were measured by varying the distance while adding a constant amount of reactant through each inlet. Straight lines were usually observed in semilogarithmic plots of parent ion counts vs the reaction distance, and the rate constants were obtained from the slope of the signal decay. Linear plots may not be observed when the parent ion is a mixture of isomers which react at different rates. For example, **2**α is reactive with CH_3OH or NO whereas **2**β is not. Significantly curved decay plots were observed for $C_8H_7^-$ (**2**α, **2**β) when excess amounts of these reactants were added. Nevertheless, rate constants for **2**α were accurately measured even in the presence of **2**β. First, an asymptotic rate constant, k', was obtained from the initial slope in the curved kinetics plot. This was achieved by reducing the reactant concentration and observing the initial part of the decay plot. The rate constant for **2**α was then derived using the relation $k = k'/f_0$, where f_0 is the initial fraction of **2**α [$=[\mathbf{2}\alpha]_0/([\mathbf{2}\alpha]_0 + [\mathbf{2}\beta]_0)$]. This fraction was determined by adding a sufficient amount of methanol to selectively remove **2**α. The error limits are usually ~10% for these measurements. When both **2**α and **2**β were reacting, we added a fixed amount of reactant from a fixed inlet while varying the injection energy to alter the $[\mathbf{2}\alpha]_0/[\mathbf{2}\beta]_0$ ratio and measuring the total depletion of **2**α + **2**β. This measurement provides relative reaction rates for **2**α and **2**β. These relative rates were converted to absolute rates by comparison with reference reactions (with measured absolute rate constants) that were examined under the same reactant conditions. Rate constants measured in this way will have larger errors (~30%) and are reported without error limits in the text.

The EBEs of **2**α (ref 7) and **3** (ref 8) have been recently measured using PES. The EBE for **1** (or adiabatic electron affinity of COT) is difficult to obtain from PES measurements because of the extremely small Franck−Condon overlap due to the very large conformational change upon transforming COT^- to COT. Instead in the present study, we determined EBE(**1**) from measurements of the equilibrium constant for $COT + O_2^- \rightleftharpoons COT^- + O_2$ using the well-established value (0.451 eV)[10] of the electron affinity of O_2. Two separate experiments were conducted to determine the equilibrium constant. One experiment involves measurements of the forward and reverse reaction rate constants for the electron-transfer equilibrium. The other involves a direct determination of the equilibrium constant by SIFT-injecting COT^- or O_2^- into the flow tube containing a COT/O_2 mixture (~1:100) while varying the total COT/O_2 density to establish equilibrium. In the latter experiment the detection conditions were adjusted so that mass discrimination between COT^- and O_2^- ions was minimal. The electron-transfer reactions of anions were examined with O_2, CS_2 (EA = 0.51 eV), SO_2 (1.107 eV), 3-$CF_3C_6H_4NO_2$ [1-nitro-3-(trifluoromethyl)benzene, 1.41 eV], and NO_2 (2.273 eV).[11]

Proton affinities (PAs) of ions were measured using proton-transfer reactions with a series of acids. The proton affinity of **2**α was precisely determined by measuring the forward and reverse reaction rate constants for the equilibrium $C_8H_7^-$ (**2**α) + $CH_3OH \rightleftharpoons C_8H_8 + CH_3O^-$. For other ions, proton affinities were determined from bracketing experiments using oxygen and sulfur acids;[11] H_2O (ΔH_{acid} = 390.8 kcal/mol), CH_3OH (380.5 kcal/mol), C_2H_5OH (377.4 kcal/mol), $(CH_3)_3COH$ (374.5 kcal/mol), CHF_2CH_2OH (366.4 kcal/mol), CF_3CH_2OH (361.9 kcal/mol), CH_3SH (356.8 kcal/mol), $C_2F_5CH_2OH$ (355.4 kcal/mol), $(CH_3)_3CSH$ (352.5 kcal/mol), H_2S (351.1 kcal/mol), CH_3COOH (348.7 kcal/mol), HCOOH (345.1 kcal/mol), and CHF_2COOH (330.8 kcal/mol). The hydrogen−deuterium (H/D) exchange reactions of ions were examined using deuterated reagents, D_2O, CH_3OD, CF_3CH_2OD, and $C_2F_5CH_2OD$. When ions **2**β and **3** undergo H/D exchange with CF_3CH_2OD, more highly exchanged products never dominate the spectrum, presumably because of a clustering loss that takes place at each collision with this reagent. In experiments with CF_3CH_2OD, therefore, highly exchanged products were carefully studied while monitoring the specific masses, optimizing the reagent concentration, and accumulating signals for longer periods (10−100 s).

Reactivities of ions were examined with NO, NO_2, SO_2, COS, CS_2, and O_2. Reactions of **2**α and **2**β are relatively difficult to examine because these ions are usually present in the flow tube as a mixture, the relative abundance depending on the injection energy. Also, the $C_8H_6^-$ (γ) ion is present at higher injection energies. Several methods and quenching reactions were employed to distinguish the reactions of each ion. For the reactions of **2**α, the ion was generated in high purity (>99%) *in the reaction flow tube* by the reaction of COT with injected

(9) Van Doren, J. M.; Barlow, S. E.; DePuy, C. H.; Bierbaum, V. M. *Int. J. Mass Spectrom. Ion Processes* **1987**, *81*, 85−100.

(10) Travers, M. J.; Cowles, D. C.; Ellison, G. B. *Chem. Phys. Lett.* **1989**, *164*, 449−455.

(11) All thermochemical data, unless otherwise noted, come from the following: Lias, S. G.; Bartmess, J. E.; Liebman, J. F.; Holmes, J. L.; Levin, R. D.; Mallard, W. G. *J. Phys. Chem. Ref. Data* **1988**, *17*, Suppl. No. 1. *NIST Negative Ion Energetics Database* (Version 3.01, 1993); NIST Standard Reference Database 19B.

Table 1. Thermochemical Data for $C_8H_n^-$ and C_8H_n

A^-	EBE (eV)	PA (kcal/mol)	$\Delta H_f(A^-)$ (kcal/mol)	$\Delta H_f(A)$ (kcal/mol)	BDE(AH) (kcal/mol)
$C_8H_8^-$ (**1**)	0.55 ± 0.02	349.9 ± 4.1	58.4 ± 0.6	71.1 ± 0.3[a]	49.1 ± 4.1
$C_8H_7^-$ (**2**α)	1.091 ± 0.008[b]	381.3 ± 2.3	86.8 ± 2.3	112.0 ± 2.3	93.0 ± 2.3
$C_8H_7^-$ (**2**β)	1.9 ± 0.5[d]	354.7 ± 5.1	33.0 ± 2.3[e]	76 ± 15[f,g]	84 ± 18[g]
$C_8H_6^-$ (**3**)	1.044 ± 0.008[c]	357.2 ± 8.3	103.6 ± 8.6	127.7 ± 8.6	67.8 ± 8.3

[a] Reference 11. [b] Reference 7. [c] Reference 8. [d] Bracketed with 3-$CF_3C_6H_4NO_2$ (EA = 1.41 eV) and NO_2 (2.273 eV). [e] Derived from the experimental value for ΔH_f(**2**α) and the calculated energy difference between **2**α and **2**β (see text). [f] Based on the estimated value for ΔH_f(**2**β). [g] The large errors mainly arise from the uncertainties in EBE obtained by bracketing measurements.

HO^- which had been formed in the source flow tube. The **2**α ions were then reacted with neutral gases added downstream. The reactivity of **2**β was examined by selectively quenching **2**α with CH_3OH or NO before **2**β was reacted with reagents of interest. Reaction products from $C_8H_6^-$ (γ) were distinguished by selectively quenching **2**α and **2**β by proton-transfer reactions with H_2S before $C_8H_6^-$ (γ) was reacted. Products from **2**α and **2**β were also examined in the absence of these additional reagents [COT for **2**α and quenching reagents for **2**β and $C_8H_6^-$ (γ)] but at different injection energies (10−40 eV), i.e., different initial abundances of **2**α and **2**β. The observed product distributions were then compared, for consistency, with those obtained in the presence of the additional reagents.

Results

This section first describes experimental results obtained for $C_8H_8^-$ (**1**), $C_8H_7^-$ (**2**α), and $C_8H_6^-$ (**3**). Results for $C_8H_7^-$ (**2**β), which is produced by collisional excitation of **2**α, are described later. Measured thermochemical data are summarized in Table 1.

Electron Binding Energy of 1. The electron binding energies (EBEs) of $C_8H_7^-$ (**2**α) and $C_8H_6^-$ (**3**) in their ground states have been recently measured using PES, and values of 1.091 eV[7] and 1.044 eV[8] were reported for **2**α and **3**, respectively.

In the present study, the EBE of **1** was determined from reaction rate measurements for both directions in the electron-transfer equilibrium $COT + O_2^- \rightleftharpoons COT^- + O_2$. Under the experimental conditions, side reactions or clustering was not observed for reaction in either direction. The forward reaction is fairly fast, and the rate constant was measured to be 8.70 ($\pm$0.70) $\times$ 10^{-10} cm^3 $molecule^{-1}$ s^{-1}, which is close to the collision limit.

The reverse reaction was found to be relatively slow [k = 1.97 ($\pm$0.20) $\times$ 10^{-11} cm^3 $molecule^{-1}$ s^{-1}]. Several different measurements were conducted to confirm the observed rate constant. Rates were measured at different injection energies for COT^- (5−25 eV). In some measurements methane or cyclohexane was added immediately after the SIFT injector to vibrationally quench COT^-. The measured rate constants were independent of these experimental conditions, suggesting that vibrationally excited COT^- ions do not contribute to the measured rate. In addition, the contribution of naturally abundant, isotopically labeled $C_8H_7^-$ ion ($^{13}C^{12}C_7H_7^-$), which has the same mass as COT^-, was found to be less than 1%. The equilibrium constant was obtained using the forward and reverse rate constants, and the electron binding energy of $C_8H_8^-$ was determined as 0.55 $\pm$ 0.02 eV.[7]

The value of EBE(**1**) obtained in this way was substantiated by separate, direct equilibrium measurements in which COT^- or O_2^- was injected into the COT/O_2 mixture. The same value of the equilibrium constant was measured when either reactant ion was injected. The measured equilibrium constant of 44 ($\pm$4) agrees well with the value from the rate measurements. The error bar for the EBE(**1**) of $\pm$0.02 eV corresponds to a factor of 2 change in the equilibrium constant and hence is fairly conservative.

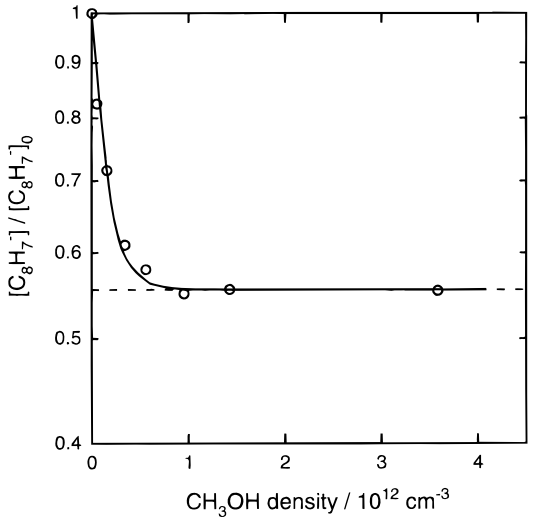

Figure 1. Kinetic plot of the loss of SIFT-injected $C_8H_7^-$ ions (injection energy 20 eV) upon reaction with CH_3OH.

Proton Affinities and H/D Exchange Reactions of 1, 2α**, and 3.** Among the several acids examined, only the conservative upper and lower brackets are reported here. The COT^- ion (**1**) reacts fairly rapidly with CH_3COOH (ΔH_{acid} = 348.7 kcal/mol) to produce CH_3COO^- while it does not react with H_2S (351.1 kcal/mol), indicating that the proton affinity of **1** lies between the values of acidities for these reagents. No H/D exchange was observed between **1** and D_2O, CH_3OD, CF_3CH_2-OD, or $C_2F_5CH_2OD$.

The $C_8H_6^-$ (**3**) ion rapidly proton-abstracts from $(CH_3)_3CSH$ (352.5 kcal/mol). Methanethiol (ΔH_{acid} = 356.8 kcal/mol) reacts moderately fast with **3** [k = 1.0 ($\pm$0.1) $\times$ 10^{-10} cm^3 $molecule^{-1}$ s^{-1}] but the formation of CH_3S^- accounted for only ~10% of the total signal loss. This suggests that the proton transfer is slightly endothermic and CH_3SH may be the upper bracket. However, the proton affinity of **3** is bracketed more conservatively with CF_3CH_2OD. While the reaction of **3** with CF_3CH_2OD was found to proceed primarily via disappearance of **3** presumably due to clustering, this reaction concurrently yielded H/D-exchanged $C_8H_{6-x}D_x^-$ products with progressively smaller amounts toward larger x. A maximum of five H/D exchanges were observed while a fully exchanged product ($C_8D_6^-$) was not detected. This extensive H/D exchange between **3** and CF_3CH_2OD suggests that the PA of **3** is lower than the value of acidity for CF_3CH_2OH (361.9 kcal/mol).

When CH_3OH was added to SIFT-injected $C_8H_7^-$ ions, two distinct components were found for $C_8H_7^-$ (Figure 1); one (defined as **2**α) reacts very rapidly to produce CH_3O^- while the other (defined as **2**β) is unreactive. The ratio of **2**α and **2**β changes dramatically upon varying the injection energy. This is clear evidence of collision-induced isomerization of $C_8H_7^-$ as detailed in the following section. The reactive component (**2**α) does not abstract a proton from H_2O, and hence the PA for **2**α is smaller than 390.8 kcal/mol (acidity of H_2O). On the

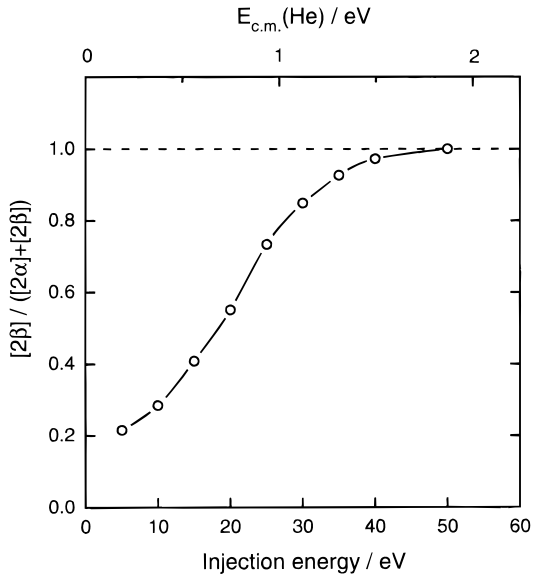

Figure 2. Isomerization fraction of $C_8H_7^-$ as a function of SIFT injection energy. The nominal center-of-mass collision energy with helium [E_{cm}(He)] is also shown.

other hand, the value for PA(**2**α) is larger than 380.5 kcal/mol (acidity of CH_3OH). Both the forward and reverse reactions were observed for the proton-transfer equilibrium $C_8H_7^-$ (**2**α) + $CH_3OH \rightleftharpoons C_8H_8 + CH_3O^-$, and in fact, the forward reaction was faster. The forward rate constant (k_f) was measured to be 1.0 (±0.1) × 10^{-9} cm^3 molecule^{-1} s^{-1}. The reverse reaction, which is slightly endothermic, generated a small fraction of CH_3O^-·COT clusters as a side product (~10%). After a minor correction for clustering, the reverse rate constant (k_r) was obtained as 2.6 (±0.3) × 10^{-10} cm^3 molecule^{-1} s^{-1}. The PA of $C_8H_7^-$ (**2**α) was determined from the equilibrium constant ($\equiv k_f/k_r$) to be 381.3 kcal/mol by assuming that $\Delta\Delta S_{Rxn}$ is negligibly small.[7] Seven H/D exchange reactions readily occur for $C_8H_7^-$ (**2**α) with D_2O, as previously observed by Hare et al.[12]

Collision-Induced Excitation of 1, 2α, and 3. The $C_8H_7^-$ ions were usually generated by reacting COT with HO^- (PA = 390.8 kcal/mol) in the ion source, and then mass-selecting and injecting them into the flow tube. The ratio [**2**α]/[**2**β], as determined by a **2**α-specific reaction with methanol, was found to change with the SIFT injection energy (Figure 2). The fraction of **2**β [$\equiv$[**2**β]/([**2**α] + [**2**β])] increased dramatically with increased injection energy until it approached unity at about 50 eV, indicating that an extensive collision-induced isomerization takes place from the **2**α to **2**β forms of $C_8H_7^-$. At higher injection energies a new CID product, $C_8H_6^-$ (γ), was also observed. This species has a reactivity distinctly different from that of $C_8H_6^-$ (**3**),[13] and the structure and formation mechanism will be discussed elsewhere.[14] The [**2**α]/[**2**β] ratio was unchanged when $C_8H_7^-$ ions were generated in the source using other deprotonating reagents, NH_2^- (PA = 403.7 kcal/mol) or CH_3O^- (380.5 kcal/mol). When $C_8H_7^-$ ions were directly generated in the reaction flow tube at 300 K by the reaction of COT with SIFT-injected HO^- ions, the $C_8H_7^-$ ions were almost exclusively in the **2**α form (>99%).

Collision-induced processes for COT^- (**1**) and $C_8H_6^-$ (**3**) appear to be relatively simple. Upon increasing the injection energy, the parent ion signals for **1** and **3** decreased until they were almost totally depleted at a potential of ~40 eV. The COT^- signal decreased more steeply than did the $C_8H_6^-$ signal. In this energy range, no product ions were observed from **1** or **3** within the detection limits. It is likely that electron detachment is the only collision-induced process for both **1** and **3**.

Reactivity of 1, 2α, and 3. Electron transfer was the only reaction observed for COT^- (**1**) with NO_2 (EA = 2.273 eV), SO_2 (1.107 eV), CS_2 (0.51 eV), and O_2 (0.451 eV). The electron-transfer reactions with NO_2 and SO_2 are very rapid whereas those reactions with CS_2 and O_2 are considerably slower. Adduct formation with NO or SO_2 was not observed for **1**.

The $C_8H_6^-$ (**3**) ions react rapidly with NO_2 and SO_2 exclusively by electron transfer. This is consistent with the PES measurement of the EBE for **3** (1.044 eV).[8] While **3** does not form a stable adduct with NO ($C_8H_6NO^-$), it reacts at a moderate rate with NO to produce CN^- [k = 3.5 (±0.4) × 10^{-11} cm^3 molecule^{-1} s^{-1}]. Despite mass discrimination against detection of CN^-, the CN^- signal accounted for a large fraction (>60%) of the signal loss of **3**. No reaction was observed with O_2 or CS_2, but **3** reacts extremely slowly with COS to produce HS^-.[15]

The $C_8H_7^-$ (**2**α) ion reacts with a variety of reactants. The reaction of **2**α with SO_2 is fast (k = 9.6 × 10^{-10} cm^3 molecule^{-1} s^{-1}), and several primary and secondary products were observed at *m/z* 64 (SO_2^-), *m/z* 65 (HSO_2^-), *m/z* 167 ($C_8H_7SO_2^-$) and *m/z* 231 [$C_8H_7(SO_2)_2^-$] with a typical abundance of 65%, 9%, 14%, and 5%, respectively.[16] Smaller amounts of *m/z* 119 ($C_8H_7O^-$, ~2%) and *m/z* 183 ($C_8H_7SO_3^-$, ~4%) were also observed. The formation of HSO_2^- was confirmed by a separate experiment in which SIFT-injected $C_8H_7^-$ (**2**α, **2**β) directly reacts with SO_2 in the absence of a possible hydrogen donor, COT (**2**β does not produce HSO_2^- from SO_2 as described later). The rapid formation of SO_2^- is consistent with the measured electron binding energy of **2**α (1.091 eV).[7] The reaction with NO_2 proceeds only via rapid electron transfer, which is also consistent with the EBE of **2**α. The **2**α ion does not react with O_2.

The ion **2**α reacts with CS_2 and COS less rapidly than with SO_2, the rate constants being 5.3 × 10^{-10} and 1.5 × 10^{-10} cm^3 molecule^{-1} s^{-1}, respectively. The reaction with CS_2 produces ionic products at *m/z* 33 (HS^-), *m/z* 57 ($HCCS^-$), *m/z* 135 ($C_8H_7S^-$), and *m/z* 179 ($C_8H_7CS_2^-$) with an abundance of 18%, 7%, 72%, and 3%,[17] and that with COS produces *m/z* 33 (HS^-), *m/z* 135 ($C_8H_7S^-$), and *m/z* 163 ($C_8H_7COS^-$) with an abundance of 31%, 9%, and 60%, respectively.

The reaction of **2**α with NO primarily leads to loss of parent ion signal, presumably due to associative electron detachment. In addition, the **2**α ion reacts with NO via sequential adduct formation at *m/z* 133 ($C_8H_7NO^-$) and *m/z* 163 [$C_8H_7(NO)_2^-$], along with minor production of CN^- (~30% of the total yield of adducts). Notably, the total rate of loss for **2**α [k_{total} = 1.1 (±0.1) × 10^{-10} cm^3 molecule^{-1} s^{-1}] is independent of the helium pressure in the flow tube (0.42−0.60 Torr), and adduct formation accounts for only ~10% of the total loss of **2**α.

Characterization of $C_8H_7^-$ (2β). In contrast to **2**α, the **2**β ion does not react with NO at a measurable rate. Neither a

(12) Hare, M.; Emrick, T.; Eaton, P. E.; Kass, S. R. *J. Am. Chem. Soc.* **1997**, *119*, 237−238.

(13) For example, $C_8H_6^-$ (**3**) abstracts a proton from $(CH_3)_3CSH$ whereas $C_8H_6^-$ (γ) does not.

(14) Kato, S.; et al. Unpublished work.

(15) The **2**β anion abstracts a proton from H_2S whereas the reaction of **2**β with COS does not yield HS^- (see the later section for **2**β), indicating that COS contains a negligible amount of an H_2S impurity. Thus, the HS^- observed in the reaction of **3** + COS is presumably a real reaction product.

(16) The experimental uncertainty for branching ratios of 10% or more is ±5%. Corrections have not been made for mass discrimination.

(17) A different product distribution was observed for the **2**α + CS_2 reaction in an FTMS experiment; i.e., $C_8H_7S^-$ and HCS_2^- were formed in a ~10:1 ratio (ref 12).

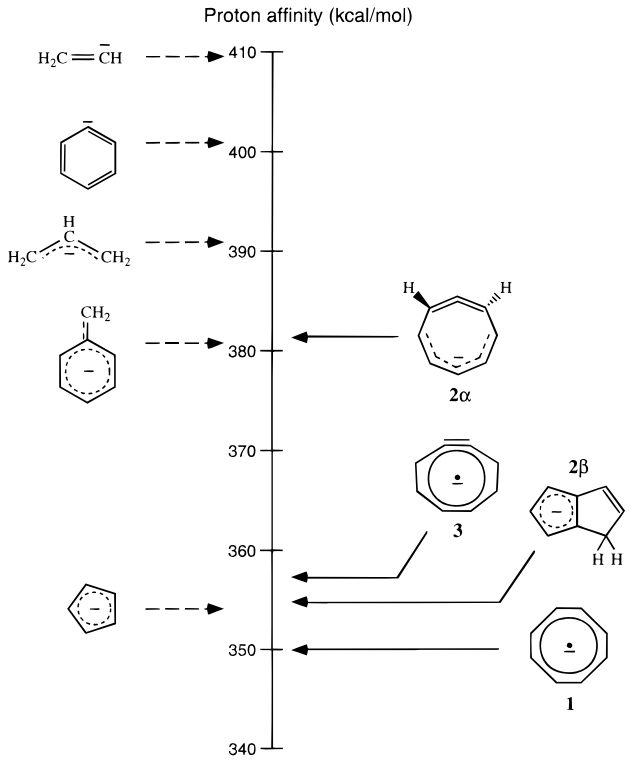

Figure 3. Gas-phase proton affinity scale for $C_8H_n^-$ (n = 6, 7, 8) and related anions.

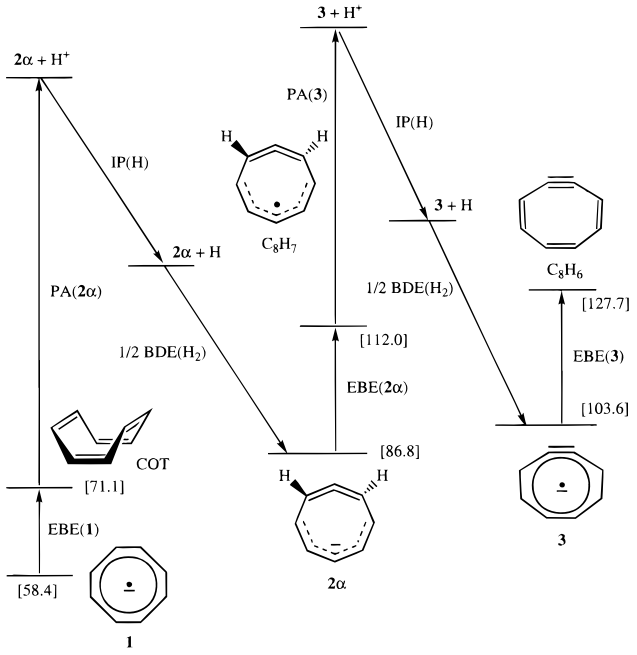

Figure 4. Energy level diagram for COT^- (**1**), $C_8H_7^-$ (**2**α), $C_8H_6^-$ (**3**), and related neutrals. Numbers in brackets represent the experimentally determined heats of formation (300 K, in kcal/mol).

decrease of the parent signal nor formation of adducts was observed for **2**β upon addition of NO in the flow tube.

The EBE of **2**β was bracketed with NO_2 (EA = 2.273 eV) and 1-nitro-3-(trifluoromethyl)benzene (NTB; 1.41 eV). While ion **2**β reacts very rapidly with NO_2 to produce a sole product, NO_2^-, no electron transfer takes place between the **2**β component of the isomer mixture (**2**α, **2**β, γ) and NTB. The proton affinity of **2**β was bracketed with $(CH_3)_3CSH$ and CH_3SH. Before the reaction, **2**α was selectively quenched with NO. While no reaction was observed with CH_3SH, **2**β abstracts a proton from $(CH_3)_3CSH$ fairly rapidly. The H/D exchange of **2**β was observed with CF_3CH_2OD. It was increasingly difficult to observe more highly exchanged products possibly because of the competitive clustering reaction as discussed above for ion **3**. Nevertheless, an exchange of up to five hydrogens was observed, and there was no evidence for further exchange.

The ion **2**β is generally less reactive than **2**α. It does not react with COS or O_2 and reacts only slowly with CS_2 to produce the adduct $C_8H_7CS_2^-$. The rate constant for the reaction of **2**β with CS_2 is only ~4% (~2×10^{-11} cm^3 molecule^{-1} s^{-1}) of that for the **2**α + CS_2 reaction. While the **2**β ion does not electron-transfer to SO_2, it forms a monoadduct at m/z 167 ($C_8H_7SO_2^-$). The HSO_2^- ion, which is a product of the reaction of **2**α with SO_2, was not observed. The reaction of **2**β with SO_2 is slower than that for **2**α, i.e., ~24% ($k = 2.3 \times 10^{-10}$ cm^3 molecule^{-1} s^{-1}) of the rate of the **2**α + SO_2 reaction.

Discussion

Thermochemical Properties of $C_8H_n^-$ and C_8H_n. Measured values for EBE and PA are tabulated in Table 1. The values of proton affinities indicate that **2**α is far more basic than other anions. Figure 3 illustrates the proton affinity scale for the anions in this study and other related anions. Although the proton affinity of **2**α (381.3 kcal/mol) is distinctly higher than those of **1**, **2**β, and **3**, it is significantly lower than that expected for typical vinylic anions [PA(CH_2=CH^-) = 409.4 kcal/mol or PA(phenyl) = 400.7 kcal/mol]. Instead, PA(**2**α) is closer to PA(allyl) (=390.8 kcal/mol) and PA(benzyl) (=380.8 kcal/mol). This suggests that the deprotonated anion **2**α is not vinylic but is additionally stabilized by delocalizing the unpaired electron over the π-system, similarly to the deprotonated anions derived from propene and toluene. The structures of **2**α and **2**β given in Figure 3 are discussed in the next section.

The EBE and PA obtained for the $C_8H_n^-$ anions can be used to calculate the heats of formation (ΔH_f) of $C_8H_n^-$ (A^-) and C_8H_n (A). First, the heats of formation of C_8H_n and $C_8H_n^-$ are related by

$$\Delta H_f(C_8H_n) = \Delta H_f(C_8H_n^-) + \mathrm{EBE}(C_8H_n^-) \qquad (2)$$

The $\Delta H_f(C_8H_n)$, in turn, is used to derive the heat of formation of the $C_8H_{n-1}^-$ ion

$$\Delta H_f(C_8H_{n-1}^-) = \Delta H_f(C_8H_n) + \mathrm{PA}(C_8H_{n-1}^-) - \mathrm{IP(H)} - (1/2)\mathrm{BDE}(H_2) \qquad (3)$$

where $PA(C_8H_{n-1}^-)$ is equal to $\Delta H_{acid}(C_8H_n)$ by definition. For the series of **1**, **2**α, **3**, and their neutrals, a reported value for ΔH_f(COT) (71.1 ± 0.3 kcal/mol)[11] is used as the reference to calculate the heats of formation for $C_8H_n^-$ and C_8H_n (Figure 4). No reported reference value is available for the family of **2**β. Instead, we estimate the heat of formation for **2**β from the value of ΔH_f(**2**α) derived above and the MO energy difference between **2**α and **2**β (53.8 kcal/mol), and use it for the reference value [ΔH_f(**2**β) = 33.0 kcal/mol] (Figure 5). Details of the MO calculation will be described in the following section. The thermochemical values obtained are summarized in Table 1. It is readily seen that the heat of formation increases in going from **1** to **2**α to **3**, for both the ion and neutral. The **2**β ion is considerably more stable than the **2**α isomer.

In addition, the homolytic C−H bond dissociation energy (BDE) of C_8H_n neutral (AH, the conjugate acid of A^-) is obtained from

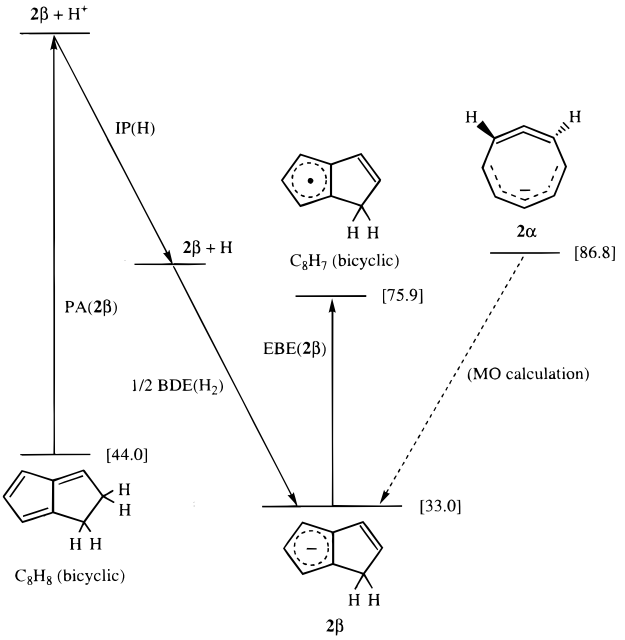

Figure 5. Energy level diagram for the $C_8H_7^-$ (**2***β*) family. Numbers in brackets represent heats of formation (300 K, in kcal/mol) as determined from both experiments and the MO energy difference between $C_8H_7^-$ (**2**α) and $C_8H_7^-$ (**2***β*).

$$\mathrm{BDE}(C_8H_n) = \mathrm{PA}(C_8H_{n-1}^-) + \mathrm{EBE}(C_8H_{n-1}^-) - \mathrm{IP(H)} \quad (4)$$

The BDE for C_8H_8 (=COT, 93.0 kcal/mol),[7] which is considerably smaller than C−H bond energies in typical sp^2 bonds,[18] is understood in terms of the stability of the C_8H_7 species due to delocalization of the radical electron over the π-system. Equations 2−4 combine 0 and 300 K quantities and do not include thermal correction terms. These terms, however, are always less than 0.3 kcal/mol (ref 22) and thus do not change the derived values in Table 1; the reported error bars include the small error which is introduced.

Collision-Induced Isomerization of 2α → 2*β*. Proton abstraction from COT yields a stable product, $C_8H_7^-$ (**2**α). The ion **2**α isomerizes to $C_8H_7^-$ (**2***β*) upon injection into the flow tube and collision with helium, the probability of isomerization depending on the injection energy. We used the MP2/6-31+G* level of theory to optimize the structures of **2**α, **2***β*, and the relevant intermediate and transition states (Figure 6).[23] Energies are calculated using the MP2/6-31+G* or semiempirical PM3 level of theory (Table 2). Corrections for zero-point energy (ZPE) and thermal energy (at 300 K) are incorporated into the calculations.

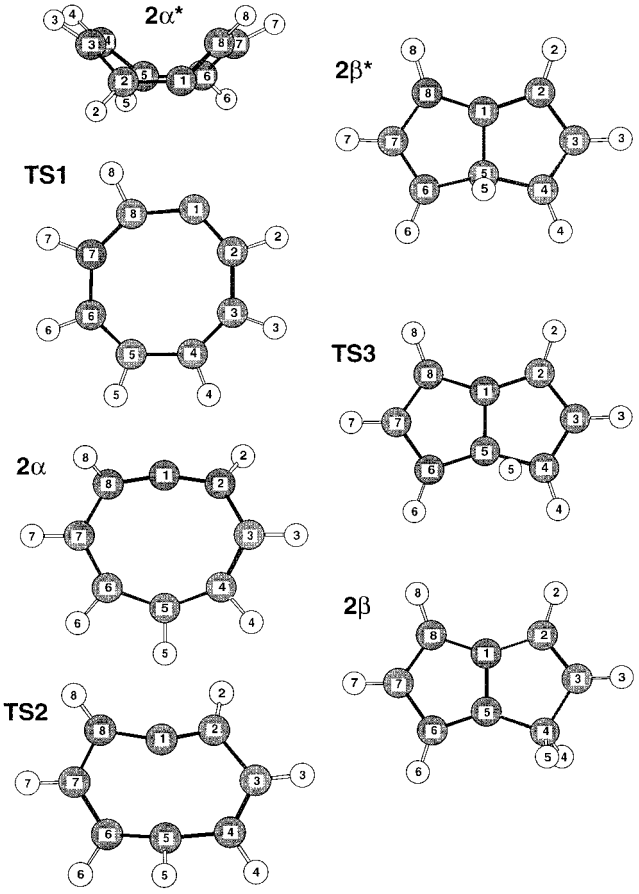

Figure 6. Structures of $C_8H_7^-$ species calculated at the MP2/6-31+G* level of theory.

The vinylic $C_8H_7^-$ ion (**2**α*) formed by proton abstraction from COT has a tublike structure very similar to that of COT with the charge localized at the site of deprotonation. The most stable form of the eight-membered $C_8H_7^-$ ring is accessed from **2**α* via a transition state (TS1) that is planar but still retains vinylic character. The optimized structure, **2**α with C_2 symmetry, is best described as a cyclic allene in a pentadienyl moiety; the C−C bonds between C1 and C2 and between C1 and C8 are the shortest, constituting a bent allenic structure whereas the C−C bonds from C3 through C7 have intermediate and similar lengths, constituting a pentadienyl moiety (Figure 7a). The dihedral angle for H2−C2−C8−H8 is nearly 90°, and the bent allenic C=C=C unit as a whole is twisted by ∼21° with respect to the C4−C5−C6 plane. The 220 cm^{-1} vibrational progression seen in the photodetachment spectrum of **2**α (ref 7) corresponds to a torsional mode of the cyclic allene in which the allenic moiety [H2−C2−C1−C8−H8] approaches a geometry closer to planarity. The highest (negative) charge density is found on C5 and then on C3 and C7, while the negative charge on the other carbons is relatively small.

The structure **2**α can be converted to a local minimum-energy [3.3.0] bicyclic structure (**2***β**) by folding along the C1−C5 axis. This process is described as the negatively charged C5 atom bridging transannularly toward the central allenic carbon. While the transition state (TS2) is still twisted, **2***β** is nearly planar. The C5 in **2***β** has substantial sp^3 character, and the charge is delocalized over nearly the entire system. The global minimum-energy [3.3.0] structure, which can be ascribed to **2***β*, is accessed by shifting the hydrogen atom on C5 toward the adjacent carbon C4, via the transition state (TS3). The optimized structure for **2***β* (Figure 7b) is planar and consists of

(18) The BDE(ethylene) and BDE(benzene) are 111.2 kcal/mol (ref 19) and 113.5 kcal/mol (ref 20) whereas those for propene and toluene are 88.8 and 89.8 kcal/mol (ref 21), respectively.

(19) Ervin, K. M.; Gronert, S.; Barlow, S. E.; Gilles, M. K.; Harrison, A. G.; Bierbaum, V. M.; DePuy, C. H.; Lineberger, W. C.; Ellison, G. B. *J. Am. Chem. Soc.* **1990**, *112*, 5750−5759.

(20) Davico, G. E.; Bierbaum, V. M.; DePuy, C. H.; Ellison, G. B.; Squires, R. R. *J. Am. Chem. Soc.* **1995**, *117*, 2590−2599.

(21) Ellison, G. B.; Davico, G. E.; Bierbaum, V. M.; DePuy, C. H. *Int. J. Mass Spectrom. Ion Processes* **1996**, *156*, 109−131.

(22) Berkowitz, J.; Ellison, G. B.; Gutman, D. *J. Phys. Chem.* **1994**, *98*, 2744−2765.

(23) *Gaussian 94*: Frisch, M. J.; Trucks, G. W.; Schlegel, H. B.; Gill, P. M. W.; Johnson, B. G.; Robb, M. A.; Cheeseman, J. R.; Keith, T. A.; Petersson, G. A.; Montgomery, J. A.; Raghavachari, K.; Al-Laham, M. A.; Zakrzewski, V. G.; Ortiz, J. V.; Foresman, J. B.; Cioslowski, J.; Stefanov, B. B.; Nanayakkara, A.; Challacombe, M.; Peng, C. Y.; Ayala, P. Y.; Chen, W.; Wong, M. W.; Andres, J. L.; Replogle, E. S.; Gomperts, R.; Martin, R. L.; Fox, D. J.; Binkley, J. S.; Defrees, D. J.; Baker, J.; Stewart, J. P.; Head-Gordon, M.; Gonzalez, C.; Pople, J. A., Gaussian, Inc., Pittsburgh, PA, 1995.

Table 2. Calculated Relative Energies for $C_8H_7^-$ Species (kcal/mol)[a]

eight-membered ring			[3.3.0] bicyclic species			[4.2.0] bicyclic species			benzene species		fulvene species	
	MP2//MP2[b]	PM3[c]		MP2//MP2[b]	PM3[c]		MP2//HF[e]	PM3[c]		PM3[c]		PM3[c]
2α*	58.3	*d*	**TS2**	69.3	76.7	(TS)	*d*		(TS)		**TS6**	74.1
TS1	83.6	70.9	**2β***	25.4	21.6	**2δ***	49.4	43.5	**2ε***	36.1	**2λ**	53.0
2α	53.8	46.7	**TS3**	38.2	47.8	**TS4**	66.9	78.6	**TS5**	79.9	**TS7**	81.0
			2β	≡0.0[f]	≡0.0[f]	**2δ**	28.6	23.6	**2ε**	14.5	**2μ***	68.2
											2μ	36.7

[a] See the text and Figures 6−8 for the structures designated by the symbols. [b] MP2/6-31+G*//MP2/6-31+G* calculations. ZPE and thermal energy (300 K) corrected. [c] Semiempirical PM3 calculations. [d] Calculations not converged. [e] Single-point MP2/6-31+G*//HF/3-21+G* calculations. ZPE and thermal energy (300 K) corrected. [f] Reference energy.

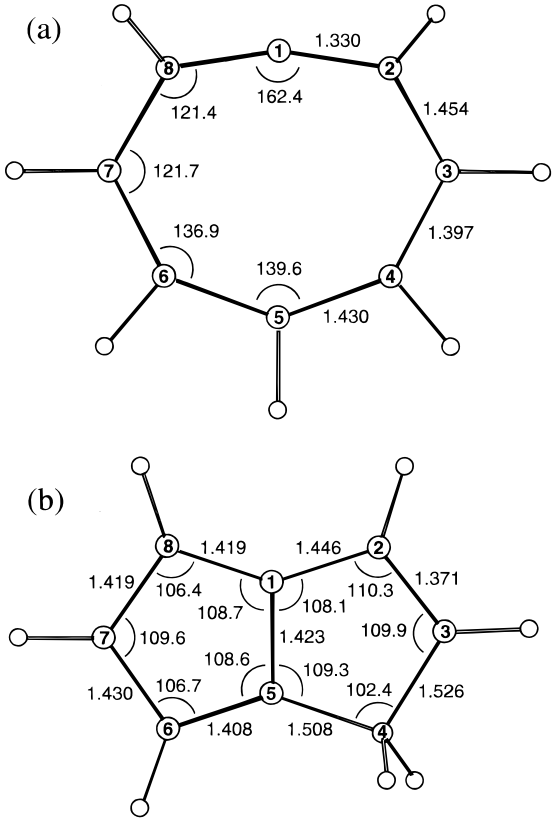

Figure 7. Structures of (a) $C_8H_7^-$ (**2α**) and (b) $C_8H_7^-$ (**2β**) calculated at the MP2/6-31+G* level of theory. Bond lengths are in angstroms, and bond angles are in degrees. The structure of **2α** has C_2 symmetry with the C8−C1−C2 plane twisted by ∼21° with respect to the C4−C5−C6 plane, while the skeletal structure of **2β** is planar.

two fused cyclopentadienyl rings. One ring has a localized C2−C3 double bond that is distinctly shorter than the others, and the shifted hydrogen atom is located on the C4 carbon with significant sp^3 character. In contrast, the other ring has C−C bonds with similar bond lengths and is highly conjugated. The transformation from **2α*** to **2β** is schematically illustrated as follows.

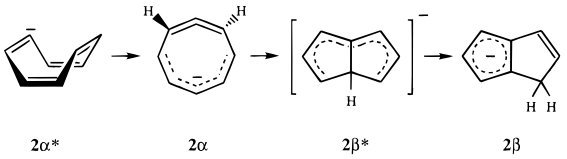

(5)

Figure 8 shows the calculated energies and schematic structures of $C_8H_7^-$ species along the reaction coordinate in going from **2α*** to **2β**. We first focus on the structure of the $C_8H_7^-$ ion obtained after deprotonation of COT. The full, rapid H/D exchange observed for $C_8H_7^-$ suggests that the carbon sites

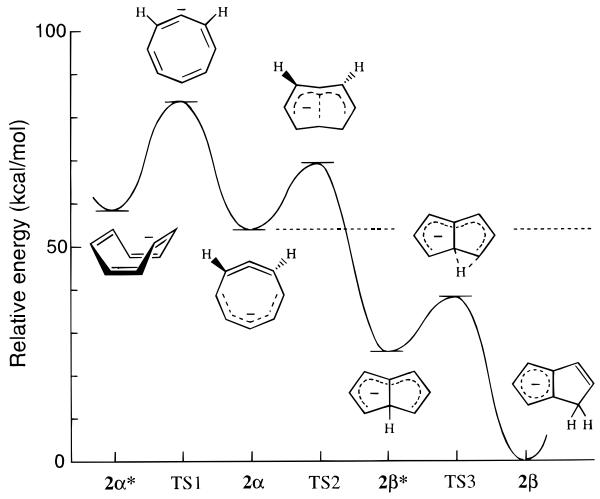

Figure 8. Relative energies (300 K) and schematic structures of $C_8H_7^-$ species obtained from MP2/6-31+G*//MP2/6-31+G* calculations. The energy for $C_8H_7^-$ (**2β**) is taken as the reference.

in the C_8H_8 neutral are almost equivalent and hence the C_8H_8 species obtained by protonation of **2α** is most likely COT. This, in turn, suggests that the $C_8H_7^-$ ion can have a similar eight-membered ring structure which is consistent with **2α*** or **2α**. According to the MP2/6-31+G* calculations (Table 2), **2α** is only 4.5 kcal/mol more stable than **2α*** while the barrier height from **2α*** to **2α** is much larger (25.3 kcal/mol). Nevertheless, the anisotropy parameter observed in PES ($\beta = -0.55$)[7] revealed that the $C_8H_7^-$ ion produced under similar conditions has a delocalized π-anionic configuration,[24] indicating that the $C_8H_7^-$ ion resulting from deprotonation of COT is **2α** and not **2α***.

Our data indicate that only **2α** is accessible by deprotonation of COT despite the relatively high barrier between **2α*** and **2α**. It is intriguing that this barrier is apparently surmounted in the nearly thermoneutral deprotonation reaction with CH_3O^- (PA = 380.5 kcal/mol). A possible mechanism involves an isomerization of nascent **2α*** to **2α** within the intermediate complex that is stabilized by an ion−dipole interaction or, more plausibly, a different bimolecular reaction path that bypasses the formation of **2α*** (eq 6).

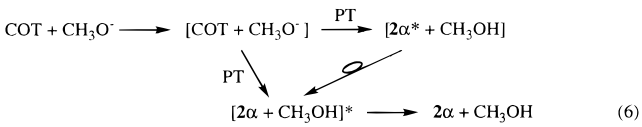

(6)

Collision-induced isomerization of **2α** to **2β** is now discussed. The first activation barrier (**TS2**) is calculated to be 15.5 kcal/mol (∼0.7 eV). The measured fraction of **2β** in the flow tube

(24) Similar negative values for β are reported for π anions such as allyl (ref 25) and benzyl (ref 26) anions whereas vinylic anions such as phenyl anion (ref 26) have positive values for β.

is almost independent of the reactant ion used in the source for deprotonation of COT [NH_2^- (PA = 403.7 kcal/mol), HO^- (390.8 kcal/mol), or CH_3O^- (380.5 kcal/mol)]. The energy released in the deprotonation reaction with NH_2^- exceeds the **TS2** energy by ~7 kcal/mol. Under the experimental conditions, however, it is not the reaction enthalpy but the collision energy that primarily determines the **2**β fraction. Despite the multiple collisions inherent in the SIFT injection, the observed behavior in the conversion of **2**α to **2**β (Figure 2) is qualitatively consistent with the calculated barrier height. Once the first barrier (**TS2**) is surmounted, **2**α is quickly transformed to **2**β, the most stable form of $C_8H_7^-$ with a remarkably low heat of formation (33.0 kcal/mol, Table 1).[27]

The ion **2**β can be viewed as the anion of fused cyclopentadienes. In fact, there are striking thermochemical similarities between **2**β and cyclopentadienide ion ($C_5H_5^-$, Figure 3). The observed PA (354.7 kcal/mol) and EBE (1.9 eV) for **2**β are very similar to those for $C_5H_5^-$ (PA = 354.0 kcal/mol, EBE = 1.786 eV). We also used semiempirical PM3 calculations to predict the EBE(**2**β). The calculations reproduce the EBE($C_5H_5^-$) reasonably well (1.74 eV), and the value for EBE(**2**β) is likewise predicted to be 1.68 eV, which is consistent with the bracketing experiment (Table 1). The above observations support the proposed cyclopentadienyl-like structure for **2**β.

The proposed [3.3.0] bicyclic structure is also consistent with the five H/D exchange reactions observed for **2**β. The MP2/6-31+G* calculations taking into account the zero-point energy (ZPE) and thermal energy (at 300 K) reveal the most stable structure for the deuterated C_8H_7D neutral to be **4a**, followed by **4b** and **4c** within ~1 kcal/mol (eq 7). While deuteration into

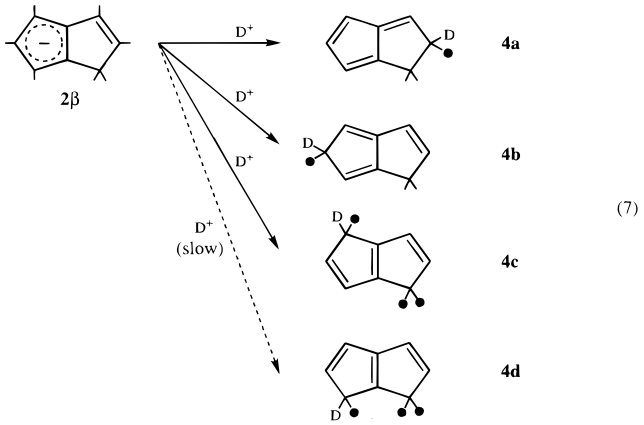

(7)

4a−**4c** and successive deprotonation facilitates a total of five H/D exchanges, the sixth exchange would be less feasible because of the relative instability of **4d** (~1.6 kcal/mol higher in energy than **4a**) and the slower H/D exchanges via this species. Recent studies on the synthesis of dihydropentalenes reported isomeric structures **4a**−**4d**, with the **4a** fulvene structure being the most stable at room temperature.[28] The values for ΔH_f(**2**β) and PA(**2**β) (Table 1) are combined to estimate the value for ΔH_f(**4a**) as 44.0 ± 7.4 kcal/mol, which agrees with an MNDO estimate of 50.8 kcal/mol by Meier et al.[28b]

Other alternative structures of **2**β are discussed here. The [4.2.0] bicyclic $C_8H_7^-$ ion (**2**δ), which is the conjugate base of bicyclo[4.2.0]octa-1,3,5-triene (**5**; ΔH_f = 48.0 kcal/mol), has only three exchangeable hydrogens and thus is ruled out as the structure of **2**β.

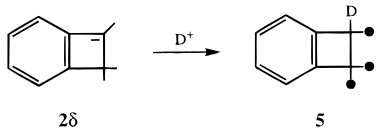

(8)

The MO calculations also support this conclusion. We calculated the structures and energies of **2**δ and its precursors **TS4** and **2**δ*.

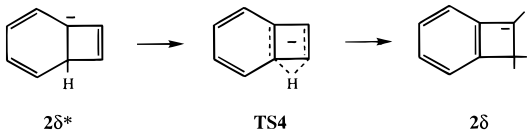

(9)

The energies for the [4.2.0] species are always 20−30 kcal/mol higher than those for the corresponding [3.3.0] species, **2**β*, **TS3**, and **2**β (Table 2). Furthermore, despite our computational effort, we find no [4.2.0]-oriented transition state that exists between **2**α and **2**δ*. The anions of styrene (**2**ϵ* and **2**ϵ) are found to be 7−9 kal/mol lower in energy than the corresponding ring-closed structures **2**δ* and **2**δ.

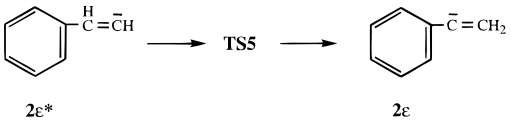

(10)

However, the measured acidity of styrene (391.0 kcal/mol)[29] clearly indicates that neither **2**ϵ* nor **2**ϵ is the structure for **2**β (PA = 354.7 kcal/mol).

Finally, ring-opened structures derived from **2**β are calculated. No reasonable structures are found for substituted cyclopentadienide ion, and instead, substituted fulvenes (**2**λ, **2**μ*, and **2**μ) are obtained by C−C bond scission of **2**β (eq 11). These

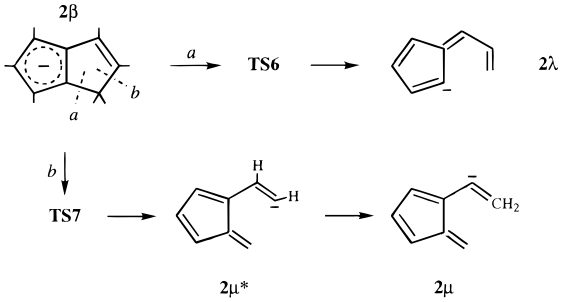

(11)

species, however, are considerably higher in energy than **2**β. It is also highly unlikely that these species behave like exact analogues of cyclopentadienide ion as ion **2**β does.

Collision-induced isomerization of anions is relatively rare. Mechanisms of classical anionic rearrangements (Wittig and anionic Claisen rearrangements,[30a−c] anionic Beckmann rearrangements,[30d] benzil/benzilic acid rearrangement,[30e] and enolate ion rearrangement[30f−h]) have been studied using collisional activation−CID detection type of instruments. A variable temperature flowing afterglow device has recently been used to measure activation energies and to characterize rearranged

(25) Wenthold, P. G.; Polak, M. L.; Lineberger, W. C. *J. Phys. Chem.* **1996**, *100*, 6920−6926.

(26) Gunion, R. F.; Gilles, M. K.; Polak, M. L.; Lineberger, W. C. *Int. J. Mass Spectrom. Ion Processes* **1992**, *117*, 601−620.

(27) The heat of formation of **2**β is estimated as 34.4 kcal/mol using PM3 calculations, in good agreement with the value in Table 1.

(28) (a) Meier, H.; Pauli, A.; Kochhan, P. *Synthesis* **1987**, 573−574. (b) Meier, H.; Pauli, A.; Kolshorn, H.; Kochhan, P. *Chem. Ber.* **1987**, *120*, 1607−1610. (c) Pauli, A.; Kolshorn, H.; Meier, H. *Ibid.* **1987**, *120*, 1611−1616.

(29) Meot-Ner (Mautner), M.; Kafafi, S. A. *J. Am. Chem. Soc.* **1988**, *110*, 6297−6303.

products in the ring opening of substituted cyclopropyl anions.[31] The [3.3.0] cyclization of **2**α to **2**β is not only a novel but a remarkable process as it contrasts with the thermal isomerization of isoelectronic COT neutral in which a Woodward−Hoffmann allowed, intramolecular cyclization to yield bicyclo[4.2.0]-octatriene is preferred. Instead, the collision-induced [3.3.0] cyclization parallels a recent observation of a low-pressure, flash pyrolysis of COT neutral that leads to [3.3.0] dihydropentalenes via a biradical mechanism.[28a,b] The anion isomerization of **2**α to **2**β is driven by a different mechanism; if this process could be duplicated in solution, it would provide novel synthetic access to bicyclic ring systems.

Chemical Reactions of $C_8H_n^-$ Ions. Experiments indicate that ion **1** (COT^-) is stable against fragmentation, and that only electron detachment, presumably converting **1** to neutral COT, takes place upon collision with helium. The radical anion **1** is notably unreactive; only electron transfer to O_2 and CS_2 and proton transfer with strong acids were observed. The ion **1** does not even form an adduct with NO, a process that is common for open shell anions. This may be understood if one considers the π-anionic nature of **1** in which the radical electron is delocalized within the π-system. The ion **1** does not react with COS or CS_2 presumably because of its low proton affinity; reactions with COS or CS_2 have been observed for anions that are strongly basic.[12,32]

The radical anion **3** ($C_8H_6^-$) is stable against fragmentation, with only electron detachment occurring upon collision with helium. The ion **3** is also relatively unreactive; the low proton affinity of **3** precludes reaction with CS_2, and only a very slow reaction was observed with COS. The absence of adduct formation with NO parallels the behavior of the radical anion of *o*-benzyne (1,2-dehydrobenzene) and contrasts with those of *m*- and *p*-benzynes.[33] Thus, ion **3** is likely a π-anion with a 1,2-dehydro-COT structure. In fact, a recent PES/MO study[8] revealed that **3** is a planar ring with a delocalized π-anion structure similar to **1**, except that it has a much shorter C−C bond at the 1,2-position with a higher bond order. Stretching of the triple bond within an eight-membered ring was observed at 2185 cm^{-1}.[8] Ion **3** exhibits a remarkable, moderately fast reaction with NO to form CN^-. A possible mechanism involves the cyclic addition of NO to the triple bond in **3** followed by rearrangements leading to the formation of CN^-, and presumably neutral products, 2,4,6-cycloheptatrien-1-one (tropone, **6**) or benzene and carbon monoxide. The energetics for these product channels indicate that the reactions are highly exothermic ($\Delta H_{Rxn} = -98$ and -114 kcal/mol, respectively). Although a similar exothermic process is, in principle, possible for *o*-benzyne ($\Delta H_{Rxn} = -117$ kcal/mol for products of CN^- and cyclopentadienone), this reaction does not occur.

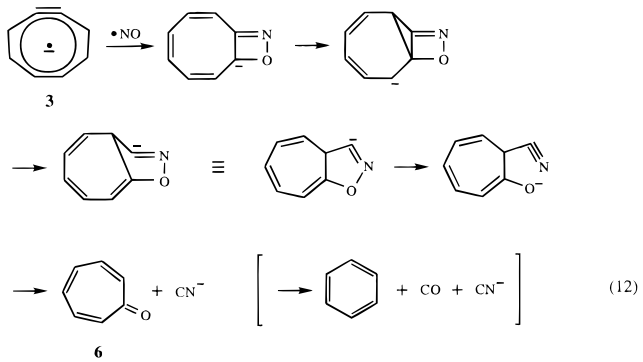

(12)

Both ions **2**α and **2**β are π-anions and are not expected to form adducts with NO. Although adduct formation is not observed for **2**β, sequential addition of NO was observed for **2**α presumably because the bent allenic bond within the ring structure provides a reactive site at the central carbon which sustains the greatest strain.

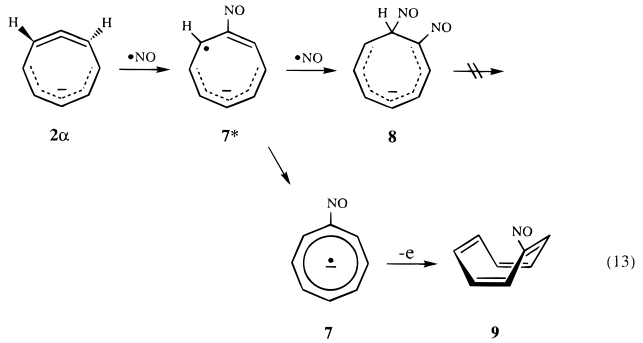

(13)

This scheme rationalizes the observed sequential addition of up to two NO molecules and the significant signal loss of the parent ion. The monoadduct (**7**) is expected to have an EBE as small as does COT^-, and the reaction exothermicity can readily detach the electron to form a closed-shell neutral product, C_8H_7NO (**9**). A similar associative detachment is reported for 2,3-dehydrophenyl anion[34] which can also yield a closed-shell neutral after detachment. Since the exothermicity is removed by release of an electron and not by collisional deactivation, the total rate constant does not depend on the helium pressure. A certain fraction of **7***, which does not undergo associative detachment, can react with another NO to form a biadduct (**8**) that no longer is reactive. Competing formation of CN^- from **2**α + NO is also explained by a plausible mechanism that involves radical attack at the strained allenic carbon.

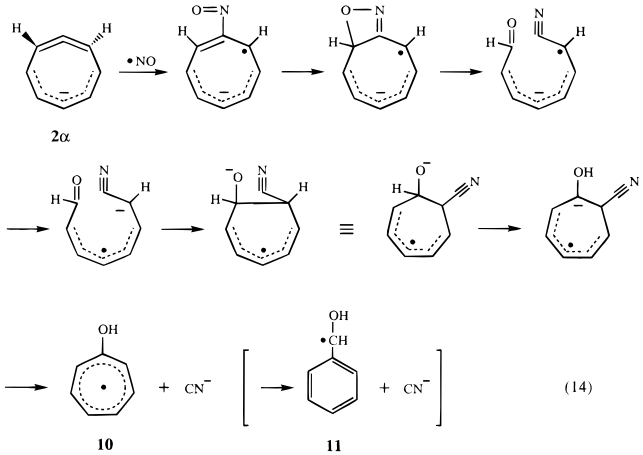

(14)

The hydrogenated tropone radical (**10**) and benzaldehyde radical (**11**) are calculated to be relatively stable [$\Delta H_f = 9.7$ and -11.0

(30) (a) Eichinger, P. C. H.; Bowie, J. H.; Blumenthal, T. *J. Org. Chem.* **1986**, *51*, 5078- 5082. (b) Eichinger, P. C. H.; Bowie, J. H.; Hayes, R. N. *Ibid*. **1987**, *52*, 5224−5228. (c) Eichinger, P. C. H.; Bowie, J. H. *J. Chem. Soc., Perkin Trans. 2* **1988**, 497−506. (d) Adams, G. W.; Bowie, J. H. *Rapid Commun. Mass Spectrom.* **1990**, *4*, 275−276. (e) Hayes, R. N.; Eichinger, P. C. H.; Bowie, J. H. *Ibid*. **1990**, *4*, 283−284. (f) Eichinger, P. C. H.; Bowie, J. H. *Org. Mass Spectrom.* **1987**, *22*, 103−108. (g) Raftery, M. J.; Bowie, J. H. *Aust. J. Chem.* **1987**, *40*, 711−721. (h) Currie, G. J.; Stringer, M. B.; Bowie, J. H.; Holmes, J. L. *Ibid*. **1987**, *40*, 1365−1373.

(31) (a) Chou, P. K.; Kass, S. R. *Org. Mass Spectrom.* **1991**, *26*, 1039−1040. (b) Chou, P. K.; Dahlke, G. D.; Kass, S. R. *J. Am. Chem. Soc.* **1993**, *115*, 315−324.

(32) (a) DePuy, C. H.; Bierbaum, V. M. *Tetrahedron Lett.* **1981**, *22*, 5129−5130. (b) DePuy, C. H. *Org. Mass Spectrom.* **1985**, *20*, 556−559. (c) Lee, H. S.; DePuy, C. H.; Bierbaum, V. M. *J. Am. Chem. Soc.* **1996**, *118*, 5068−5073.

(33) Wenthold, P. G.; Hu, J.; Squires, R. R. *J. Am. Chem. Soc.* **1994**, *116*, 6961−6962.

kcal/mol, respectively, at the PM3 level] owing to the delocalized radical electrons. The reaction enthalpies are estimated to be −81 and −102 kcal/mol, respectively.

Sulfur dioxide forms adducts with anions **2**α and **2**β. For the reaction with **2**β, a single SO_2 can bind at the anionic cyclopentadienyl site to form a stable product, $C_8H_7SO_2^-$. Adduct formation with **2**α can initiate from addition of SO_2 at the strained allenic carbon site (eq 15). The formation of a

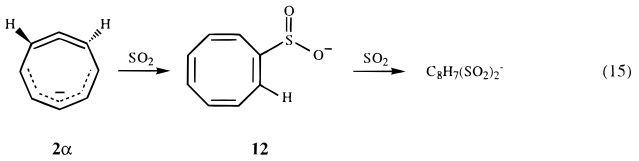

(15)

biadduct for **2**α and not for **2**β suggests an intermolecularly stabilized covalent structure for the biadduct, although it is also possible that the biadduct is a cluster, with the second SO_2 interacting with the sulfonate ion moiety of **12**. The formation of HSO_2^- (and presumably C_8H_6) from **2**α may be surprising because the calculated value for the hydride affinity of C_8H_6 (**3**) (76 ± 9 kcal/mol, from Table 1) is greater than that for SO_2 (63 kcal/mol).[11] This suggests that an isomerized, lower energy C_8H_6 product must be formed from this reaction. The formation of HSO_2^- cannot occur for **2**β for which the reaction enthalpy for the product pair with HSO_2^- and presumably pentalene is estimated to be significantly endothermic.

The reaction of **2**α with COS and CS_2 proceeds via both sulfur atom abstraction and adduct formation. Sulfur atom abstraction from COS or CS_2 has been observed for carbanions that are highly basic, e.g., N≡C−CH_2^- (PA = 372.8 kcal/mol),[32a] CH_2=C=CH^- (380.5 kcal/mol),[32b] quadricyclanide ion (403.0 kcal/mol),[32c] and cubyl anion (404 kcal/mol).[12] This accounts for the absence of sulfur abstraction reactions for **2**β. For the reaction of **2**α with CS_2, abstraction of sulfur [$C_8H_7S^-$ (**13**), 72%] and the consecutive elimination of $HCCS^-$ (7%) account for the majority (79%) of the reaction products (eq 16). With a PM3-calculated value for $\Delta H_f(HCCS^-)$ of −13.5 kcal/mol, the reaction enthalpy for the elimination channel is estimated to be exothermic by ∼45 kcal/mol. Elimination of HS^- from $C_8H_7S^-$ is not feasible on energetic grounds. Adduct formation and the consecutive elimination of HS^- are minor processes with CS_2 (eq 17). Once the adduct is formed, however, this reaction is quite exothermic and a large fraction of nascent adducts undergo dissociation to yield HS^- (18%), with only 3% remaining as the adduct (**14**). The reactions of **2**α with COS can proceed via similar mechanisms but with a significantly different product distribution. The overall reaction rate constant is also smaller for COS than for CS_2. Formation of adduct ($C_8H_7COS^-$, 60%) and the consecutive elimination of HS^- (31%) account for the majority (91%) of the reaction. The nascent adduct with COS is less internally excited than that with CS_2, thereby potentially leading to more stabilization rather than further dissociation. Sulfur abstraction ($C_8H_7S^-$, 9%) is unexpectedly slow with COS, although this reaction is generally more exothermic than that with CS_2 because of the elimination of CO instead of CS. This behavior parallels that observed for the reaction of quadricyclanide ion with CS_2 and COS,[32c] suggesting a kinetic barrier to sulfur abstraction from COS.

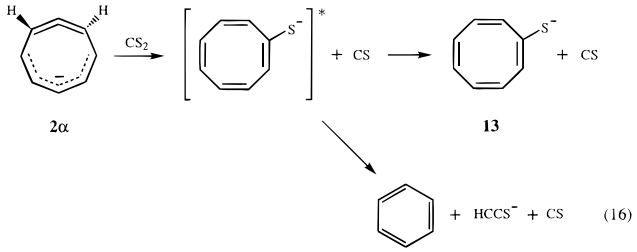

(16)

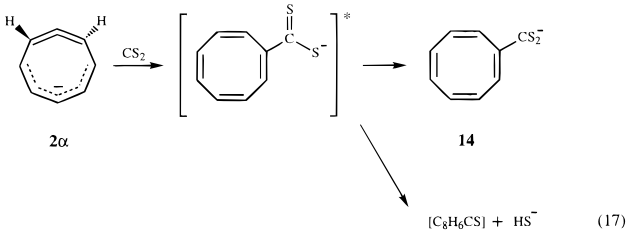

(17)

Conclusions

The structures, energetics, and chemical reactions of COT^- (**1**), $C_8H_7^-$ (**2**α), $C_8H_7^-$ (**2**β), and $C_8H_6^-$ (**3**) were studied using the SIFT technique and MO calculations. The adiabatic electron affinity of COT was unambiguously determined as 0.55 ± 0.02 eV. Heats of formation for the anions and related neutrals, along with the C−H bond dissociation energies for the conjugate acids, were also determined from measurements of proton affinities and electron binding energies.

Collisional excitation of the eight-membered ring species **1**, **2**α, and **3** induces different reactions. While π-radical anions **1** and **3** undergo electron detachment upon collision with helium, anion **2**α undergoes a novel isomerization to a different anionic species, **2**β, at relatively low collision energies. At higher energies, loss of hydrogen atom to yield the $C_8H_6^-$ (γ) species, which has a reactivity distinctly different from that of $C_8H_6^-$ (**3**), was also observed. The anion **2**α is not a vinylic anion but a novel, π-electronic system with a cyclic allene structure in a pentadienyl moiety. The anion **2**β is a relatively stable [3.3.0] bicyclic species (ΔH_f = 33.0 kcal/mol) with EBE and PA very similar to those for cyclopentadienide ion.

The high proton affinity, high heat of formation, and strained cyclic allene structure in **2**α give rise to a variety of chemical reactions, e.g., sulfur abstraction and adduct formation with CS_2 and COS, and sequential adduct formation with NO and SO_2. Other anions are relatively unreactive. However, anion **3** reacts with NO at a moderate rate to yield CN^-.

Collision-induced isomerization of **2**α to **2**β with transannular bond formation is a remarkable process. Duplication of this isomerization process in solution would provide entry into bicyclic ring systems that pose significant synthetic challenges. The structure of $C_8H_6^-$ (γ) is particularly intriguing; this species may be the radical anion of pentalene if it retains the skeletal structure of **2**β. Characterization of this species is currently underway.

Acknowledgment. We gratefully acknowledge support of this work by National Science Foundation Grants CHE-9421747 and CHE-9421756. We also thank Dr. Paul G. Wenthold for helpful discussions.

JA972628O

(34) Hu, J.; Squires, R. R. *J. Am. Chem. Soc.* **1996**, *118*, 5816−5817.